VISIBLE BIDIRECTIONAL REFLECTANCE MEASUREMENTS FOR TWO RELEVANT SNOW SURFACE MORPHOLOGIES

Daniel A. Miller[1*] and Brad T. Stanton[1]

[1]Department of Civil Engineering, Montana State University, Bozeman, MT, USA

ABSTRACT: The influence of near surface changes on visible reflection characteristics is important to many aspects of snow science as it represents a major energy source to the snowpack and a primary interface to the environment. Snow radiative transfer models often utilize spheres of equivalent specific surface area (SSA) while more complex models strive to predict snow's directional reflectance properties requiring accurate bidirectional reflectance values for various crystal habits. However, few studies in this area exist and none focus specifically on surface hoar.

Microstructural changes due to near surface metamorphism, traced by crystal size and type, alter snow's solar bidirectional reflectance. Specifically, the bidirectional reflectance distribution of the snow's surface before and after surface hoar growth will be quantifiably different when viewed in the visible wavelengths, thereby possibly allowing the remote detection of surface hoar presence.

Surface hoar was grown on rounded grains in a lab setting. Temporal changes in crystal mass and specific surface area were documented using x-ray computed tomography, while meteorological instrumentation recorded environmental conditions. A spectrometer was used to measure bidirectional reflectance factors (BRF) both before growth (rounded grains) and after growth (surface hoar) from 42 different incident lighting and viewing geometries.

Analysis of the results revealed three primary conclusions: 1) In the transition from rounded grains to surface hoar, mean BRF values (essentially albedo) decrease slightly ($\leq 2.9\%$) likely due to an increase in grain size; 2) Accompanying surface hoar growth showed an increase in SSA and a departure from Lambertian scattering. That is, surface hoar has significantly brighter peak values and significantly darker minimum values than rounded grains; 3) Incident lighting and viewing geometries at which these maximum and minimum BRF values occur show no discernible pattern.

KEYWORDS: surface hoar, snow albedo, bidirectional reflectance.

1. INTRODUCTION

A central challenge faced in researching the optical properties of snow is the extensive diversity of possible crystal habits. To address this challenge, a common simplification in radiative transfer models is to utilize an *optically equivalent grain*—a mathematical construct that approximates the complex shape and size of an actual snow crystal by defining a spherical grain with an equivalent *specific surface area* (SSA)—i.e. surface area to volume ratio (Wiscombe and Warren, 1980; Li and Zhou, 2004; Domine et al., 2006; Picard et all. 2008). While necessary for models using Mie scatter theory, the optically equivalent sphere neglects many of the crystal features that affect its directional scattering properties and is primarily useful in hemispherically averaged radiative quantities such as irradiance or albedo (Jin et al., 2008).

A more appropriate approach for capturing the effects of crystal habit on the angular distribution of reflected light is a comprehensive multi-angle study using various incident and observer angles. Multi-angle studies often report results in terms of a *bidirectional reflection distribution function* (BRDF, f_r) or a *bidirectional reflectance factor* (BRF, R). As the name implies, a BRDF "describes the scattering of a parallel beam of incident light from one direction in the hemisphere into another direction in the hemisphere" (Nicodemus et al., 1977 and Brugge et al., 2000). Mathematically, it is the ratio of incident irradiance E (W m^{-2}) from a single direction to the radiance L (W m^{-2} sr^{-1}) exiting the surface in a single direction. This ratio is a function of reflectance azimuth (θ_r) and zenith (ϕ_r) angle as well as incident zenith (θ_i) and azimuth (ϕ_i) angle and, finally, wavelength (λ) (Figure 1).

* *Corresponding author address:*
Daniel Miller, 205 Cobleigh Hall, PO Box 173900 Bozeman, MT 59717-3900;
tel: 406-994-6118; fax: 406-994-6105;
email: dan.miller@ce.montana.edu

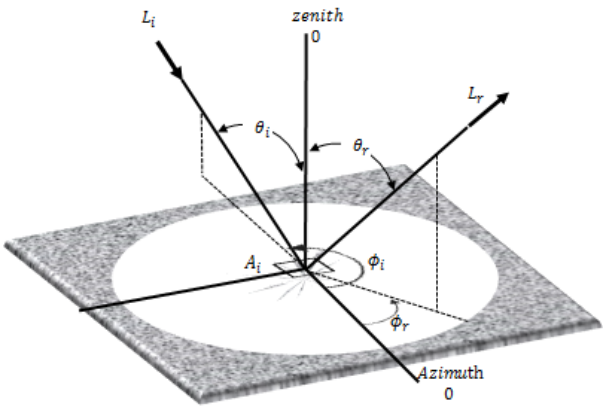

Figure 1. Reflectance azimuth (θ_r) and zenith (ϕ_r) angle as well as incident zenith (θ_i) and azimuth (ϕ_i) angle. In this study, 0 azimuth is defined relative to the incident light such that ϕ_i = 180°.

Because it is a ratio of infinitesimal properties, the BRDF cannot be measured directly (Schaepmann-Strub et al., 2006). In studies where reflection is measured directly, results are reported in terms of a BRF value, a unitless ratio of power $\Phi_{r,snow}$ reflected from the snow surface to the power $\Phi_{r,ideal}$ reflected from a commercially available Lambertian reference standard such as Spectralon,

$$R = \frac{\Phi_{r,snow}(\theta_i, \phi_i, \theta_r, \phi_r)}{\Phi_{r,ideal}(\theta_i, \phi_i)}. \quad (1)$$

In practice, field studies using the sun as the illumination source have both a direct and diffuse (due to Rayleigh scattering in the atmosphere) component (e.g. Leroux et al. (1998), Aoki et al. (2000), Painter and Dozier (2004), Li and Zhou (2004), Bourgeois et al. (2006)). These studies often report a *hemispherical directional reflectance factor* (HDRF) to indicate the result includes incident light scattered by the atmosphere. HDRF values, which depend on daily atmospheric conditions, are difficult to compare to BRDF. In a study that uses a similar methodology as the current study, Dumont et al. (2010) looked at the directional dependence of four different grains (dendritic fragments, clustered rounded grains, melt freeze crusted grains, new wet snow) over a wide range of lighting and viewing geometries. They concluded that both grain size and shape have an effect on the reflectance distribution (primarily in the NIR and longer wavelengths) but that it is difficult to predict. Further, they were able to distinguish a recognizable reflectance pattern for elongated or faceted shapes. Specifically, they noted darkening at viewer grazing angles in situations of near nadir illumination as well as strong forward-scatter peak in the NIR wavelengths for all grain types. However, Dumont's study did not specifically address surface hoar.

Several distinct themes can be seen in these studies: 1) snow in the UV/VIS wavelengths appears far more Lambertian than snow in longer wavelengths; 2) albedo decreases with increasing grain size; 3) snow tends to demonstrate a strong forward-scatter peak at large incident light angles. 4) grain habit plays a role but is not well understood.

This study's hypothesis is that microstructural changes due to the growth of faceted surface hoar crystals at the snow's surface, will alter visible bidirectional reflectance as compared to rounded grains. Specifically, it is postulated that the BRF of the snow's surface before and after surface hoar growth will be predictably and quantifiably different. Surface hoar was developed in a laboratory setting using rounded grains as the starting morphology. Optical reflectance properties were then examined to establish bidirectional reflectance before and after surface hoar growth.

2. MEHODOLOGY

All experiments were conducted in a walk-in environmental chamber at Montana State University's Snow Science Engineering Research Facility (SSERF). This chamber allowed control of meteorological conditions such that surface hoar could be grown on a 30x30cm snow surface. In addition, a built in solar simulator eliminated excess atmospheric scatter allowing the reporting of directional (as opposed to hemispherical-directional) data.

A single test consisted of recording BRF values from 42 different lighting/viewing geometries (21 forward scatter and 21 backscatter) both before and after surface hoar growth. In addition, microscopic images and CT scans where used to document crystal type before and after surface hoar growth. In total, three of these tests were conducted to verify repeatability, resulting in three sets of optical data on rounded grains and three sets of optical data on a-axis dominate surface hoar.

In the cold chamber, a Stellarnet Inc. Black Comet-HR spectrometer with a holographic concave grating covering 200-1100 nm ranges was used to capture spectral data from the snow surface. A custom hemispherical gantry was built to support the spectrometers probe (Figure 2). This goniometer allowed the probe to be positioned at viewer zenith (θ_r) and azimuth (ϕ_r) ranging from $\sim 0^\circ$ to

75° and a full $360°$ respectively. A metal-halide solar simulation lamp provided a spectral distribution comparable to the sun (in the range between 280—2480 nm). Since the light source was built into the ceiling and could not be moved, sun geometry was controlled by tilting the snow surface with respect to the light as illustrated in Figure 2. Incident zenith angles utilized in this study were $15°$, $30°$, and $45°$. Finally, the common convention of defining a solar incident plane such that the sun is always at an incident azimuth angle of $180°$ was used.

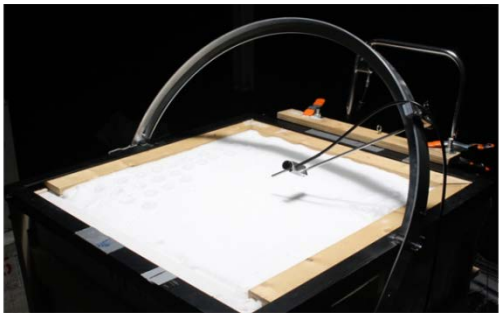

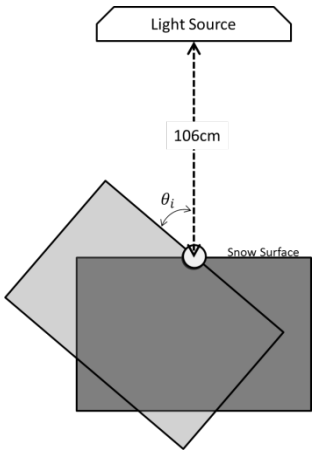

Figure 2. Upper: Goniometer and Spectrometer Configuration. Lower: Sun angle θ_i was varied by tilting the snow surface with respect to the fixed light source.

The snow samples were prepared and surface hoar was grown with the procedures outlined in Stanton et al (2012). To ensure accurate, high quality documentation of surface crystal type as well as to document changes in microstructural parameters that might affect optical results, computed tomography (CT) images were taken before and after each optical test. Detailed processing and representative images are shown in Stanton et al (2012).

3. RESULTS AND DISCUSSION

BRFs were collected on each test at 42 different view geometries. Figure 3 depicts a representative BRF for all 42 sampled geometries from one test (each line represents a different lighting and viewing configuration). No legend is provided as it would be impractical for 42 values; instead this data is meant to reveal general trends. Note that perfect Lambertian scatter would be represented on the plots as BRF value of 1 across all wavelengths. In subsequent discussion, BRF values at 510nm (green light) are used as a representative value for the scattering behavior of light in the visible wavelengths. This is a justifiable since BRF values at a given viewer/incident geometry are similar across the visible bandwidth. Therefore, any visible wavelength will demonstrate similar anisotropy in scatter.

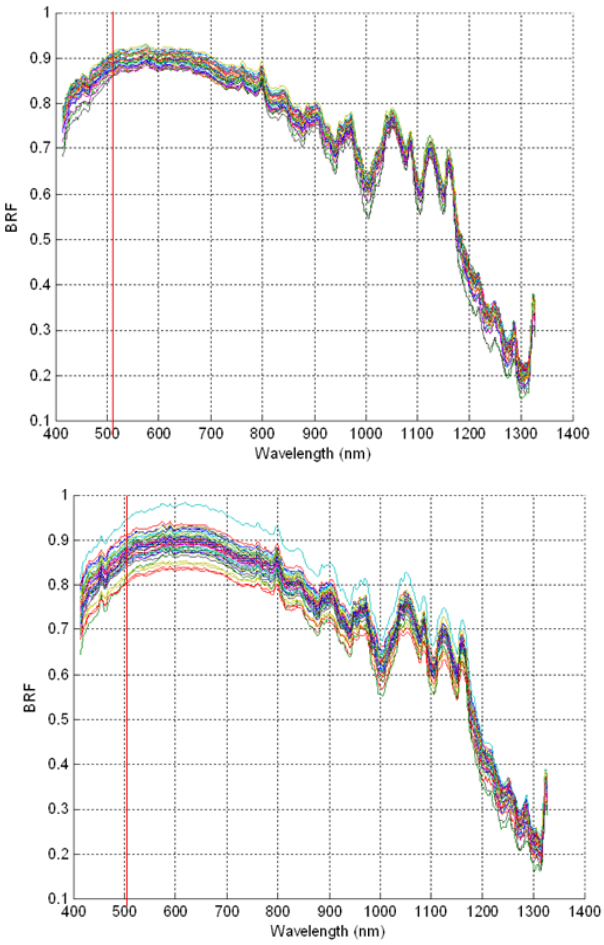

Figure 3. Representative BRF as a function of wavelength. Each line represents a different lighting and viewing geometry. Initial rounded form (top) and surface hoar (bottom). Red line marks 510 nm.

Table 1 summarizes BRF characteristics at 510nm. The distinct features in this set of data are the slight decrease in mean BRF (essentially albedo) and significant increase in BRF standard deviation and range between initial form and final form indicating surface hoar scatters light in a less Lambertian manner than rounded grains.

Test 3 Rounded Grains		**Test 3 Surface Hoar**	
Mean	0.884	Mean	0.870
Median	0.886	Median	0.873
Std. Dev.	0.014	Std. Dev.	0.028
Range	0.052	Range	0.142
Maximum	0.858	Maximum	0.807
Minimum	0.911	Minimum	0.949

Table 1. Descriptive statistics for BRF values across all geometries at 510 nm from Figure 3.

Several observations concerning the above data are consistent with previous studies and lend credibility to the results. Notably, in the visible wavelengths, snow is highly reflectivity with BRF values dropping off distinctly as wavelength increases toward the NIR. In the visible wavelengths the BRF values varied by less than ~17%, regardless of grain type or lighting/viewing geometry. These relatively small variations in BRF are consistent with Dumont et al. (2010) and are predicted by Warren (1982).

More importantly, the data also reveal surface hoar to be a less Lambertian reflector than rounded grains. From the initial form to the surface hoar form, there is a distinct spreading of the BRF in all three tests. That is, when the data is looked at as a whole, a greater range of BRF values is seen for surface hoar than for rounded grains. Quantitatively, there is a 12.8%, 66.3%, and 172% increase in the range of BRF values in the transition between rounded grains and surface hoar in each of the three tests respectively. This indicates surface hoar reflectance is significantly less Lambertian than rounded grains. In the three tests, the smallest change in BRF range from rounded grains to surface hoar, also experienced very little change in specific surface area (SSA). This suggests a link between SSA and BRF values based on grain type in the visible spectrum. Increasing SSA is accompanied by a brightening of the brightest points in the hemisphere and decrease in the darkening of the darkest points in the hemisphere. More succinctly, increasing SSA is accompanied by increasing departure from Lambertian scatter.

Warren (1982) suggests, in the NIR, larger gain size means that a photon must transverse more ice before encountering a diffractive surface and the chance to be ejected from the snowpack. As such, it has a higher chance of being absorbed than for small grains where the number of scattering events, and thus the probability of being ejected, is greater. Concisely stated, in the NIR, smaller grains are more reflective than larger grains. This effect is less pronounced in the UV/VIS, where the low abortion of ice makes it less sensitive to grain size. Accordingly, at 510 nm, grain size should have less of an effect on the reflectance than in the NIR.

One would then expect smaller BRF values for surface hoar (the physically larger grain) than for rounded snow (the physically smaller grain). In the experiments, there is a slight decrease (Table 2) in *mean* BRF between rounded grains and surface hoar. However, the change is generally small.

Test #	**Mean BRF**	**% Change**
1 RG	0.892	-2.9%
1 SH	0.867	
2 RG	0.873	-0.1%
2 SH	0.872	
3 RG	0.884	-1.6%
3 SH	0.870	

Table 2. Mean BRF values from tests 1, 2, and 3 and percent change from rounded grains to surface hoar at 510 nm.

The decrease in mean BRF is likely accounted for by the increase in grain size. However, accompanying this slight decrease in mean, there is a large increase in the standard deviation of the mean—as much as 98.2% (Table 3).

Test #	BRF STD Dev	% Change
1 RG	0.013	47.8%
1 SH	0.019	
2 RG	0.018	69.0 %
2 SH	0.031	
3 RG	0.014	98.2%
3 SH	0.028	

Table 3. Standard deviation and percent change in standard deviation of BRF values from rounded grains to surface hoar in each of the three tests at 510 nm.

This change in grain size does not account for the general increase in the range and standard deviation that occurs in the transition from rounded grains to surface hoar. More likely this is due to grain shape (crystal habit) and indicates that the bright points get brighter and the dark areas get darker when viewing surface hoar as compared to rounded grains. That is, as surface hoar develops, SSA increases and the reflected light departs from Lambertian scatter.

Next, at what geometries do we find the minimum and maximum BRF values for rounded grains and surface hoar and are these geometries predictable from test to test? The 42 geometries from each test were examined in detail. In agreement with previous studies, the data demonstrate darkening near the edges at nadir incident angle and a forward-scatter peak along the solar principle plane. More importantly, the data also indicates no discernible geometric pattern in BRF values. There was no discernible pattern predicting where the maximum or minimum bright point will occur spatially. An observer inspecting a field of surface hoar will likely find it brighter or darker at certain viewing angles as compared to rounded snow (which appears more Lambertian), but predicting the geometry of the bright and dark points is not possible with the data collected here. The data and detailed analysis is available in Stanton (2013).

4. CONCLUSIONS

Conclusions of this study suggest a possible optical signature unique to surface hoar. As surface hoar develops, SSA increases and the reflectance from the snow surface becomes less and less Lambertian. While there is a slight decrease in overall albedo, likely due to the increase in grain size, it is not significant enough to account this departure from Lambertian reflectance. Likely grain shape is playing a primary role in the scattering properties of the snow. However, the data suggests that the viewer/incident geometry at which point the BRF value is maximum or minimum cannot be predicted. That is, while an observer of a field of surface hoar will notice locations at which the snow appears brighter and other locations at which the snow appears darker, the exact positioning of those light and dark points cannot be predicted. Further, for every dark point observed there will be a corresponding light point somewhere elsewhere in the hemisphere; therefore, albedo changes very little.

ACKNOWLEDGEMENTS

This work was supported by The Department of Civil Engineering at Montana State University, National Aeronautics and Space Administration (NASA), the Montana Space Grant Consortium, National Science Foundation (award 1014497) and the Murdock Charitable Trust.

REFERENECES

Aoki, T., T. Aoki, M. Fukabori, A. Hachikubo, Y. Tachibana, and F. Nishio (2000). “Effects of snow physical parameters an spectral albedo and bidirectional reflectance of snow surface.” Journal of Geophysical Research 105:10219-10236.

Bourgeois, C.S., P. Calanca, and A. Ohmura (2006). “A field study of the hemispherical directiona reflectance factor and spectral albedo of dry snow.” *Journal of Geophysical Research* 111: 1-13.

Bruegge, C.J., J.V. Martonchik, and A.H. Strahler (2000). “A review of reflectance nomenclature used in remote sensing.” *Remote Sensing Reviews* 19: 9-20.

Domine, F. R. Salvatori, L. Legagneux, R. Salzano, M. Fily, R. Cassacchia (2006). “Correlation between the specific surface area and the short wave infrared (SWIR) reflectance of snow.” *Cold Regions Science and Technology* 46: 60-68.

Dumont, M., O. Brissaud, G. Picard, B. Schmitt, J.C. Gallet, and Y. Arnaud. (2010). “High-accuracy measurements of snow bidirectional reflectance distribution function at visible and NIR wavelengths—comparison with modeling results.” *Atmospheric Chemistry and Physics*. 10: 2507-2520.

Jin, Z., T.P. Charlock, P. Yang, Y. Xie, and W. Miller (2008). “Snow optical properties for different particles shapes with application to snow grain size retrieval and MODIS/CERES radiance comparison over Antarctica.” *Remote Sensing of Environment* 112: 3563–3581.

Leroux, C., j.L. Deuze, P. Goloub, C. Sergent, and M. Fily (1998). “Ground measurements of the polarized bidirectional reflectance of snow in the near-infrared spectrum domain: comparison with model results.” Journal of Geophysics Research 103: 19721-19731.

Li, S., & X. Zhou (2004). “Modeling and measuring the spectral bidirectional-reflectance factor of snow-covered sea ice: An intercomparison study.” *Hydrology Processes* 18: 3559−3581.

Nicodemus, F.E., J.C. Richmond, J.J. Hsia, I.W. Ginsberg, and T. Limperis (1977). “Geometrical considerations and nomenclature for reflectance.” NBS Monograph 160, National Bureau of Standards, US Department of Commerce, Washington, D.C.

Picard, G., L. Arnaud, F. Domine, M. Fily (2008). “Determining snow specific surface area from near-infrared reflectance measurements: numerical study of the influence of grain shape.” *Cold Regions Science and Technology* 56: 10-17.

Schaepman-Strub, G., M.E. Schaepman, T.H. Painter, S. Dangel, J.V. Martonchik (2006). “Reflectance quantities in optical remote sensing—definitions and case studies.” *Remote Sensing of Environment*. 103: 27-42.

Stanton, B.,(2013) “Visible Bi-directional reflectance measurements for rounded grains and surface hoar snow crystal morphologies”, Masters’ Thesis, Montana State University, May 2013.

Stanton, B., D.A. Miller and E.E. Adams, “Analysis of Surface Hoar Growth Under Simulated Meteorological Conditions”, *International Snow Science Workshop*, Anchorage, AK, September 2012

Warren, SG. (1982). “Optical properties of snow.” *Reviews of Geophysics and Space Physics*. 20: 67-89.

Warren, S.G., and W.J. Wiscombe (1980). “A model for the spectral albedo of snow I, snow containing atmospheric aerosols.” *Journal of Atmospheric Science* 37: 2712-2733.

Warren, S.G., and W.J. Wiscombe (1980). “A model for the spectral albedo of snow II, snow containing atmospheric aerosols.” *Journal of Atmospheric Science* 37: 111-44.